Journal of Materials Chemistry C

Accepted Manuscript

This article can be cited before page numbers have been issued, to do this please use: A. Rubino, M. Anaya, M. E. Calvo and H. Míguez, *J. Mater. Chem. C*, 2016, DOI: 10.1039/C6TC00663A.

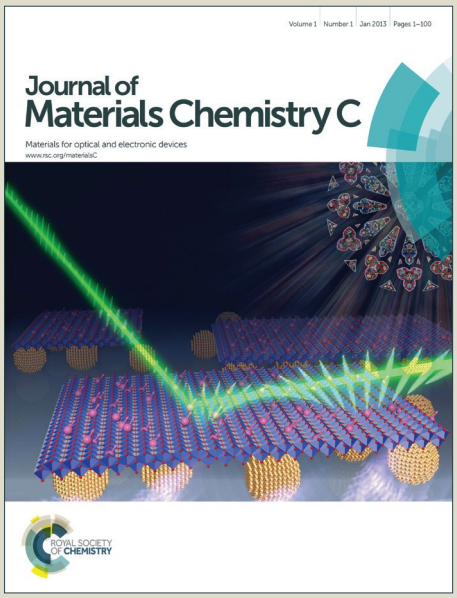

ROYAL SOCIETY OF CHEMISTRY

www.rsc.org/materialsC

View Article Online
DOI: 10.1039/C6TC00663A

Journal Name

ARTICLE

Solution Processed High Refractive Index Contrast Distributed Bragg Reflectors

Received 00th January 20xx,
Accepted 00th January 20xx

DOI: 10.1039/x0xx00000x

www.rsc.org/

Miguel Anaya, Andrea Rubino, Mauricio E. Calvo*, Hernán Míguez*

We have developed a method to alternate porous and dense dielectric films in order to build a high refractive index contrast distributed Bragg reflector (DBR) capable of reflecting very efficiently in a targeted spectral range employing a small number of layers in the stack. Porous layers made of SiO_2 nanoparticles and compact sol-gel processed TiO_2 layers are sequentially deposited. The key to the preservation of porosity of every other layer during the deposition process is the use of a sacrificial layer of polystyrene that prevents the infiltration of the interstitial voids between nanoparticles with the homogeneus solution of TiO_2 precursors. Our approach allows preparing a series of DBRs operating along the whole visible spectral range. Reflectance values as high as 90% are achieved from only seven layers. The particular distribution of porosity along one direction gives rise to an interesting interplay between the optical properties of the system and the vapor pressure in the surrounding atmosphere, which we foresee could be put into practice in gas sensing devices.

Introduction

Superior performance, low-cost processing and ease of integration are *sine quibus non* conditions for novel materials to be used in advanced technologies amenable to mass production. In this context, solution processes dielectric nanostructures for light management have increasingly attracted interest due to their potential to improve the performance of optoelectronic devices.[1-3] Within the large family of dielectric optical materials, distributed Bragg reflectors (DBRs) are probably among the first and most basic designs that have been employed for this purpose.[4] A DBR consists typically in two different compounds alternately stacked to produce a periodic modulation of the refractive index (*n*) in one dimension of the space. As a consequence of this, strong interference phenomena occur and selective light reflection at certain wavelengths ranges is achieved.[5] Both the spectral position and the intensity of the reflectance peak (or Bragg peak) depend on the thickness, refractive index and number of the slabs deposited. The use of DBRs is nowadays spread in numerous fields, being found in many systems as passive elements acting like frequency selective mirrors, filters or optical resonators.[6,7] By integrating them with light absorbing or/and emitting materials, DBRs find very relevant applications in the fields of lighting and solar energy, where they are used to enhance light harvesting or photoluminescence processes.[8-13]

The larger the dielectric contrast between alternate layers is, the lower the number of slabs required in the stack to achieve a certain reflectance value and the wider the spectral width at which it occurs. For DBRs operating in the visible range, silicon oxide (SiO_2) and titanium oxide (TiO_2) are typical materials of choice due the large refractive index difference they present. An alternative approach to high refractive index contrast DBRs is based on the alternation of layers with different porosity. This idea has been put into practice for the realization of DBRs made of a variety of compositions,[14-20] including those in which a single compound is used.[21-23] Techniques employed to achieve this alternation of porosities are diverse and include, among others, physical vapour deposition,[14,15,20,21] electrochemical acid etching,[22] and liquid processing.[16-18,24] Besides, the presence of controlled porosity in DBRs has enormously expanded their range of applications in many relevant fields in recent years.[25] For example, opto-electronic and optofluidic devices may benefit from the diffusion of species through a network of accessible and interconnected voids within a mirror or optical resonator.[18,26-32]

From the point of view of wet chemistry, the combination of different porosities in the same stack is a challenge that has been mainly addressed following two different strategies. In one approach, porosity can be created or increased within the low refractive index layer by the inclusion of a porogene. This compound remains in the layer avoiding the infiltration of a freshly deposited top layer until it is removed by thermal or chemical treatment. After porogene elimination, an open interconnected[33-35] or an occluded and not accessible porosity is obtained.[36] On the other hand, suspensions with nanoparticles in different aggregation state can be used as

[a] Instituto de Ciencia de Materiales de Sevilla, Consejo Superior de Investigaciones Científicas-Universidad de Sevilla, Calle Américo Vespucio 49, 41092 Sevilla, Spain. E-mail: h.miguez@csic.es ; mauricio.calvo@icmse.csic.es.

† Footnotes relating to the title and/or authors should appear here.
Electronic Supplementary Information (ESI) available: [SEM image of TiO_2/MgOF system, reactive concentrations table, XRR data, reflectance of DBR under liquid infiltrations]. See DOI: 10.1039/x0xx00000x

View Article Online
DOI: 10.1039/C6TC00663A

precursors to alternately deposit thin layers with different porosity.[17,37,38] Nanoparticle layers are advantageous because of their stability against disassembly under solvent immersion, allowing the subsequent deposition of a new layer of nanoparticles. When nanoparticles of very small size are deposited on top of a layer of large nanoparticles, the risk of losing dielectric contrast can be prevented by using a sacrificial polymer that impedes their interpenetration.[39]

Herein, we explore the limit of this sacrificial polymer approximation to build DBRs with maximized reflectance. We describe a general synthetic procedure to obtain high refractive index contrast DBRs based on the alternation of dense sol-gel processed TiO_2 films and highly porous SiO_2 nanoparticle layers. During the deposition of the liquid precursors of the dense layers, the porosity of the low refractive index ones is preserved by prior filling of the interstitial voids with a sacrificial polymer that is eliminated at the end of the process. The key to create a stack of high structural quality lies in preventing the infiltrating polymer to create a film above the protected nanoparticle layer, since that would cause the collapse of the structure when the polymer is eventually removed. By this means, we show that it is possible to build multilayers displaying an intense reflectance band of above 90% employing only a small number of dielectric layers in the stack. Such band can be tuned to sweep the whole visible region of the electromagnetic spectrum by adjusting the thickness of the layers. While the potential of these new materials in the field of emerging photovoltaic devices has been recently demonstrated, here we focus on the analysis of the evolution of their optical properties to varying environmental conditions. Vapour diffusion and condensation properties of the two types of layers present in the stack determines the response of the system and can be potentially put into practice in new sensing devices.

Results and discussion

The choice of TiO_2 and SiO_2 to build colored DBRs with enhanced refractive index contrast is supported by the fact that they present one of the highest and lowest, respectively, refractive indexes among all transparent materials in the visible range. Besides, they present other attractive properties such as ease of processing, low toxicity and low cost, which make them amenable to device integration and mass production. Dense TiO_2 layer precursors were prepared by a sol-gel route and deposited employing a spin-coating technique, as described in detail in the Experimental section. By this means we expected to attain a refractive index of around n=2.2 in the center of the visible spectrum, as it has been reported in the literature.

Regarding the low refractive index material, as far as we know, the transparent porous layer with the lowest refractive index reported is one based on MgOF prepared by wet deposition.[40] However the integration of this material in a DBR is seemingly not feasible due to its collapse during the sequential stacking required to build the DBR, as we demonstrate in the supplementary information (Figure S1). Hence, in order to improve with respect to the value attainable with dense silica prepared by sol-gel (n=1.45), we employed a strategy based on the deposition of SiO_2 nanoparticles that we have previously demonstrated that may allow reaching values as low as n=1.22.[41] In fact, thin optical quality layers with n <1.25 are scarce in the field of solution processed materials, some examples being CaF_2,[42] MgF_2[43] , whose preparation is also not easily compatible with the processing of a multilayer, or mesostructured SiO_2 layers, whose preparation involve the use of organic supramolecular templates and lengthy stabilization treatments.

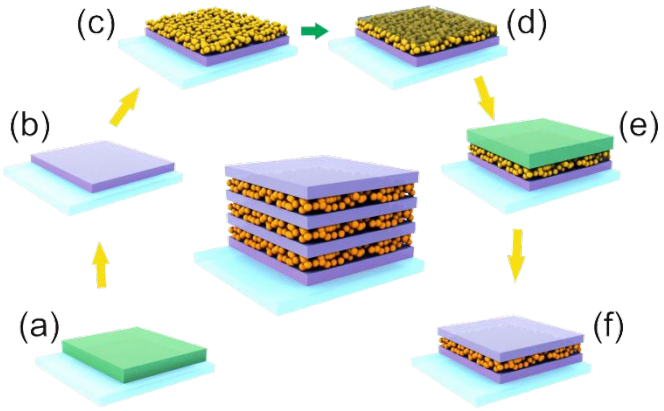

Fig. 1 Scheme of the deposition pathway that leads to a high porous/low porous multilayer stack, (a) deposition of TiO2 layer, (b) thermal treatment, (c) deposition of SiO2 particles, (d) protection of SiO2 particles with polystyrene, (e) deposition of TiO2 layer, (f) thermal treatment. The process is repeated following these steps until the desired number of layers is achieved.

In contrast, thin layers of SiO_2 nanoparticles have been proven to be robust enough to support the stacking of different types of particles and can be easily deposited by spin coating or dip-coating.[12,17,44] However, their use faces the problem of infiltration when combined with the deposition of a continuous phase from a liquid dispersion. In order to overcome this obstacle, we propose a procedure based on the temporary filling of the interstitial void between nanoparticles with a polymer, as it is described in the scheme of Figure 1. After the deposition and the thermal treatment of a first dense TiO_2 layer (Figures 1a and 1b), we stacked a layer of SiO_2 nanoparticles (Figure 1c). Next, we placed some drops of a polystyrene (PS) solution and started the spin coating. Polystyrene is forced to fill the voids of the SiO_2 nanoparticulated layer and blocks the access to the pore network (Figure 1d). As polystyrene is insoluble in isopropanol, the precursors of a new TiO_2 layer deposited on top of this hybrid SiO_2-PS layer cannot percolate through them (Figure 1e). Finally, a thermal shock treatment at 500°C further densifies the TiO_2 layer and causes the thermal decomposition and removal of the PS from the SiO_2 layer pores (Figure 1e). The parameters related to the deposition of the PS layer have been appropriately set to obtain a complete filling of the porous underlying layer and, at the same time, minimize the accumulation of polystyrene on the top. Otherwise, the eventual thermal annealing of that excess of polystyrene can compromise the mechanical stability of the ensemble.

View Article Online
DOI: 10.1039/C6TC00667A

Sequential repetition of these steps until the desired number of slabs is deposited leads to the formation of a multilayer.

In Figure 2 we show secondary electron (SE, Figures 2a and 2c) and backscattered electron (BSE, Figures 2b and 2d) images simultaneously taken from the same area of a cross section of a nine-layer DBR made by alternating compact TiO_2 and porous SiO_2. Figure 2a and b disclose smooth and continuous interfaces between both types of layers with high uniformity at the microscale. Each type of layer can be recognized by their different morphology in SE images as well as by their different response in BSE ones. In the latter, brighter regions indicates the presence of elements of higher atomic number. High magnification images (Figures 2c and 2d) reveal the spherical morphology of the SiO_2 nanoparticles and the homogeneity and continuity of the compact TiO_2 layer, as well as the absence of interpenetration between both types of layers.

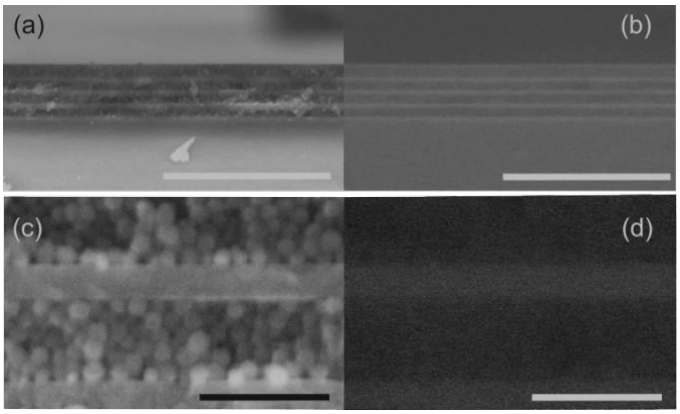

Fig. 2. Cross section images obtained by FESEM of a TiO_2 / np-SiO_2 multilayer structure. Images were obtained using secondary (a) and backscattered (b) electrons detectors. Scale bar is 2 μm in both images. Magnification of a section of the top images is shown in (c) and (d). Scale bar is 200 nm for both images.

X-ray reflectivity (XRR) characterization was employed to evaluate the density of the layers. Although it was not possible to obtain reliable data for the case of the silica layers, XRR data taken from TiO_2 layers allowed estimating a density of 3.11 g/cc, in very good agreement with reported data for dense TiO_2.[45] Full details are provided in the Supporting Information section and Figure S2 therein.

As we mentioned above, the modulation of the refractive index along one dimension of the space leads to the occurrence of strong interference effects. When these effects are spectrally located in the visible region of the electromagnetic spectrum, bright colors can be seen by the naked eye. In Figure 3, a picture of a series of seven layer DBRs supported on glass slides is displayed, the color gamut covering the whole visible range.

The evolution of the reflectance of this type of DBRs with the number of layers can be seen in Figure 4. It can be observed that with only 3 layers ($TiO_2/SiO_2/TiO_2$, blue solid line) the measured reflectance reaches values as high as 50%, increasing up to 75% and 90% when two and four extra layers are added, respectively (red and black solid lines). Porosity of the individual layers of the DBR can be estimated through the fitting of these reflectance spectra using a code based on a full vector wave transfer matrix approximation.[46] The simulated spectra (dashed lines in Figure 4) are in fair agreement with the experimental ones. Refractive indexes of 2.12 and 1.29 for TiO_2 and SiO_2 layers, respectively, were considered for $400nm<\lambda<800nm$ for these calculations. This implies that the refractive index contrast is 0.83, one of the highest values achieved for a solution processed DBR, which are 0.87 and 0.84, as reported in ref. 34 and 36, respectively. Please notice that the estimated refractive index for the SiO_2 layer is slightly larger than the expected one, which ranged between 1.23 and 1.25.[17,18] This may indicate that a small percentage of the interstitial volume in the SiO_2 layer is filled by the liquid dispersion of TiO_2 precursors, which could be due to incomplete filling of such volume with polystyrene or to permeation of the precursors through the sacrificial layer. We can estimate that only 5% of the free space in SiO_2 layers is filled with TiO_2. It is important to remark that the optical constants of both types of layers remain unaltered as the DBR is constructed. This conclusion demonstrates that the minor infiltration of the SiO_2 layer is not an accumulative process but it takes place only when each new SiO_2/TiO_2 interface is created.

In Figure 5, we plot the experimental reflectance spectra obtained by a series of 7-layer-1DPCs prepared combining non-porous TiO_2 and highly porous SiO_2. It can be observed that the values of the maximum oscillates between 86% and 96%.

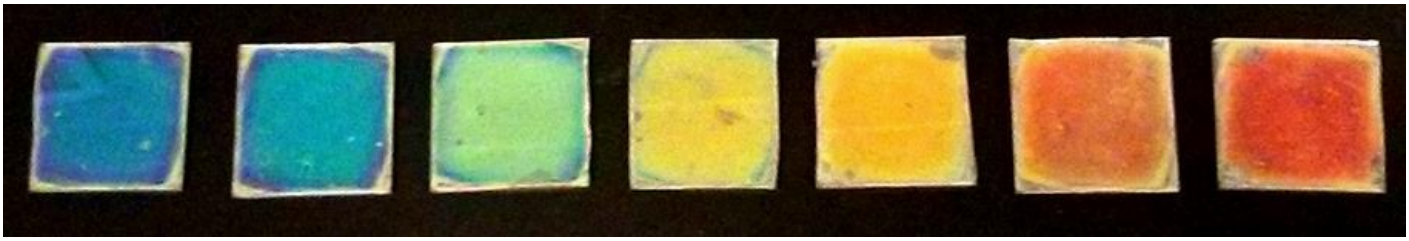

Fig. 3: Digital camera images obtained from a series of high porosity SiO_2/low porosity TiO_2 distributed Bragg reflectors prepared with SiO_2 suspension deposited by employing different concentrations and final rotation speed.

View Article Online
DOI: 10.1039/C6TC00663A

Journal Name

ARTICLE

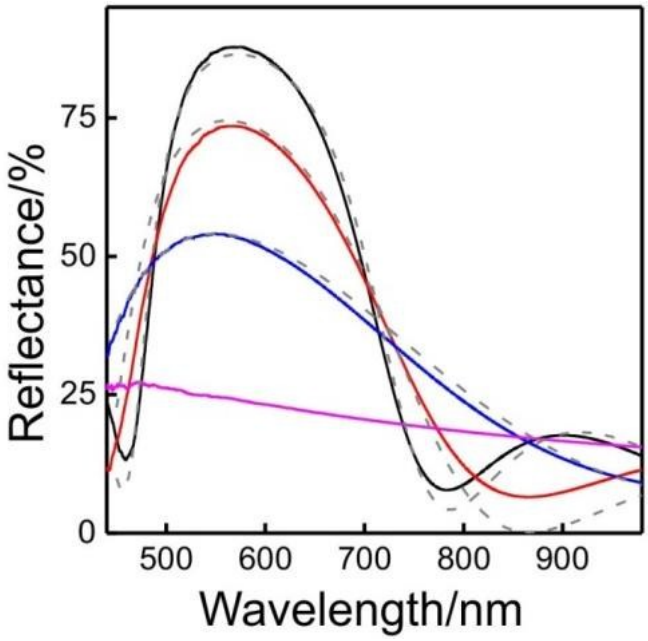

Fig. 4. Evolution of the reflectance spectra as the number of stacked layers increases. Experimental data are plotted in solid line being the number of layers: 1 (violet line); 3 (blue line); 5 (red line); 7 (black line). Theoretical calculated spectra are depicted in dashed grey lines

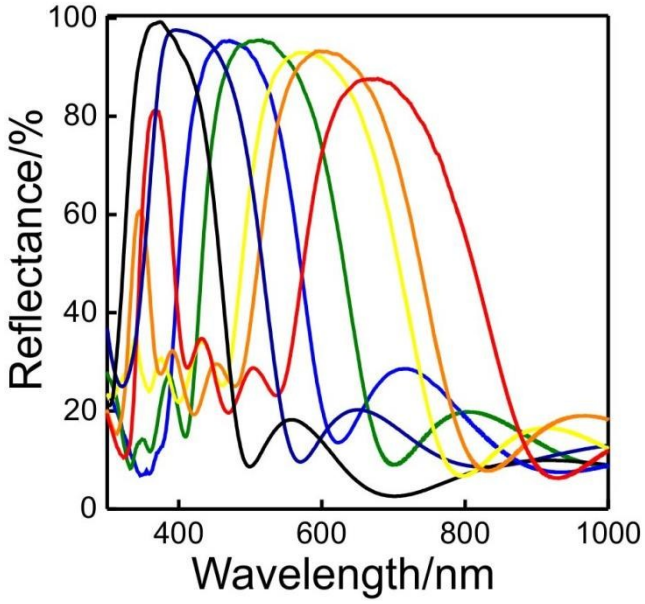

Fig.5. Reflectance spectra of a series of high porous SiO_2/low porous TiO_2 DBRs built with 7 layers starting with TiO_2. Samples were obtained using different conditions by means: T1 and [SiO_2]=1.0% (black line); T2 and: [SiO_2]=1.0% (violet line), [SiO_2]=1.5% (blue line), [SiO_2]=2.0% (green line), [SiO_2]=2.5% (yellow line), [SiO_2]=3.0% (orange line), [SiO_2]=3.5% (red line).

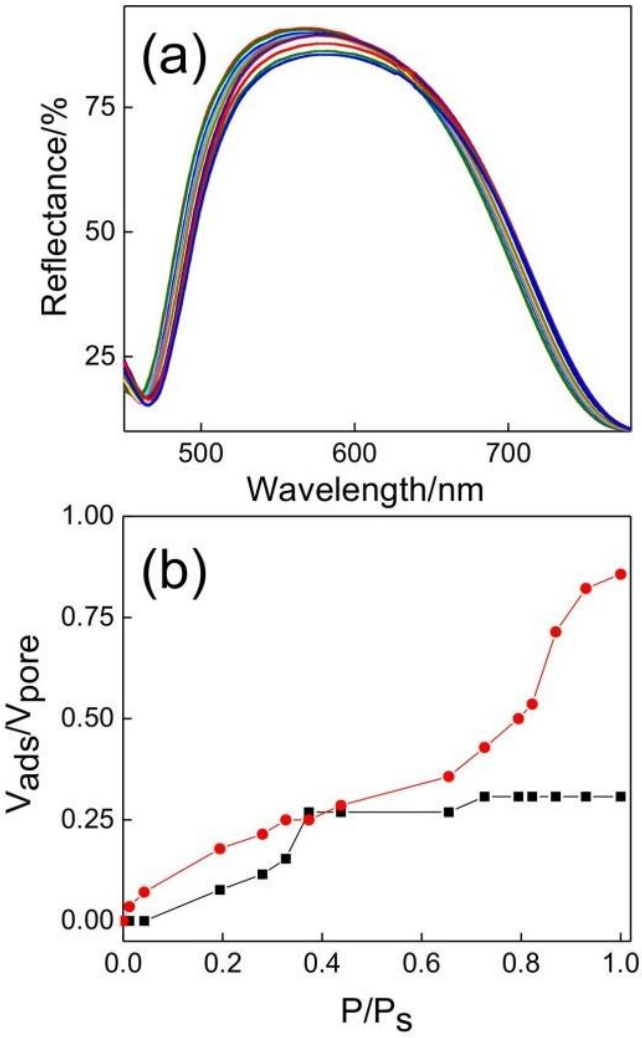

Fig.6. (a) Reflectance spectra of a DBR exposed to different isopropanol vapor pressures obtained at gradually increasing pressures after reaching equilibrium. (b) Pore filling fraction for each type of layer, namely TiO_2 (black squares) and SiO_2 (red squares), at different isopropanol vapor pressure. Isopropanol pressure is normalized to saturation value (P/P_S).

On the other hand, the value of the normalised spectral width of the Bragg peak, calculated as $\Delta\lambda/\lambda_{Bragg}$ (being $\Delta\lambda$ the FWHM and λ_{Bragg} the spectral position of the Bragg peak) was found to be near 0.37, similar to what the best efforts done in the field in the past have achieved.[34,36]

It is interesting to notice that the porosities estimated from the refractive index values attained employing Bruggeman's model are 12% and 35% for TiO_2 and SiO_2, respectively. This means that the compact TiO_2 slab is not dense *stricto sensu*, but it presents certain porosity not observable under the

scanning electron microscope that must therefore correspond to the presence of micropores. In order to further analyse the interstitial sites present in the DBRs we employed a porosimetry technique based on specular reflectance.[47] It has been shown that when the open pores of a multilayer displaying a Bragg peak are gradually infiltrated by a guest compound, the induced changes in the refractive index of the layers give rise to a red-shift in the spectral position of the Bragg peak and a modification of its intensity.[48] By monitoring *in situ* these variations as we rise and lower the pressure of a vapor (isopropanol in our case) in a chamber in which the DBR is placed, we can obtain a complete adsorption-desorption isotherm cycle, from which very detailed information on the pore structure can be attained.[16] The evolution of the Bragg peak for a complete adsorption/desorption cycle is depicted in Figure 6a. By fitting these spectra we can evaluate the pore volume that is progressively filled in each type of layer present in the sample as vapor pressure increases. Results are shown in Figure 6b. Abrupt changes in the spectral position and intensity of the Bragg peak are observed for P/P_s>0.65 and correspond to vapor condensation within the SiO_2 layer pore network, which is made of almost monodisperse nanoparticles hence presenting a narrow pore size distribution. Contrarily, adsorption within the much more compact TiO_2 lattice takes place smoothly, confirming the previously suggested hypothesis of the presence of micropores. The response to changes in the ambient atmosphere also demonstrates that this microporosity is partially open.

These DBRs can also be infiltrated from the liquid phase. As example, we took some organic solvents commonly employed in the preparation of optoelectronic devices by liquid processing. Figure S4 shows the reflectance spectra of a 1DPC before and after the infiltration with three different liquids. The experiment is done in such a way that the only possible entrance to the structure is through the less porous TiO_2 layer. The liquid drop is placed on top of the stack and at its center, hence avoiding any potential infiltration by the side. Like in the case of gas phase compounds, as the liquids fill the voids in the structure, the Bragg peak shifts to longer wavelengths, being this change proportional to the refractive indices of the guest fluid.

Conclusions

We have demonstrated a solution processed route to achieve high refractive index contrast distributed Bragg reflectors. These types of systems present the ability to reflect over 90% of the incoming light at the desired spectral ranges employing only a few periods in the stack. These highly reflecting dielectric structures are less than 500 nm thick. We have also shown that these characteristics are accompanied by the possibility of infiltrating gas or liquid phase compounds into the photonic structure, giving rise to spectral variations on their optical response. These entire attributes make the system herein reported a potential candidate to be integrated in technologies that make use of thin films, such as photovoltaics or sensing, in order to provide them with enhanced optical performance.

Experimental

Liquid dispersions

TiO_2 precursor dispersion synthesis was made by adding 0.254 ml (named T1) or 0.381 ml (named T2) of titanium tetraisopropoxide (TTIP, Sigma Aldrich, 377996) under strong stirring to a solution that contains 0.034 ml of water, 0.034 ml of a 2M hydrochloric acid in 3.38 ml of ethanol. Once TTIP is added, the resulting mix is kept under stirring during one hour before use.

SiO_2 suspension was purchased from Sigma-Aldrich (Ludox TMA 420859). Particle suspension is diluting in ethanol to reach desired suspensions with final concentrations between 1% and 4%.

Polystyrene solution is made by dissolving an appropriate amount of solid polystyrene (Aldrich, 182427) in toluene.

Multilayer deposition

A spin coating route combined with thermal treatment is chosen in order to control the thickness and the deposition of SiO_2 and TiO_2 layers, and to control the infiltration of the SiO_2 porous layer by polystyrene. The scheme of the process is detailed in Figure 1. In a typical multilayer process 200 µl of a TiO_2 precursor dispersion is dropped on top of a clean substrate (quartz, glass slide or silicon). Final rotation speed is set at 2000 rpm. This first layer is treated at 400ºC during 10 minutes. Next a layer of SiO_2 nanoparticles (150 µl) is deposited from the suspension on top of the first TiO_2 layer and spun at final speeds from 3000 rpm to 5000 rpm depending on the desired thickness. For each deposition step, the acceleration step is set in order to achieve in one second the final rotation speed. After that, a 150 µl of the polystyrene solution (0.5% wt. toluene solution) is spin casted to the preformed multilayer structure. The amount of infiltrated polystyrene was controlled for each DBR through the final rotation speed, which was varied from 2000 rpm (thicker SiO_2 layers) to 4000 rpm (thinner SiO_2 layers). In Figure S4 we show how the optical properties of a DBR are affected by the different polystyrene loads achieved. Then, a layer of TiO_2 is deposited following the same protocol described before. The process is repeated until a desired number of layers is stacked

Structural Characterization

FESEM images of the multilayers films deposited onto silicon were taken by using a microscope Hitachi 5200 operating at 5 kV

XRR data were carried out using a Panalytical X'PERT PRO system in reflection mode. A $Cu_{k\alpha}$ radiation (40mA, 45 KV) and a θ range from 0^o to 9^o were employed to obtain the reflectivity data.

Optical Characterization

Reflectance spectra from 500 nm to 1200 nm were performed using a Fourier Transform spectrophotometer (Bruker IFS-66 FTIR) attached to a microscope and operating in reflection mode with a 4X objective with 0.1 of numerical aperture (light cone angle ±5.7º). The reflectance spectra in the 300 nm to 500 nm range were measured using an UV-Vis spectrophotometer (UV-2101PC, Shimadzu) attached with an integrating sphere. All spectra were

View Article Online
DOI: 10.1039/C6TC00663A

corrected by a calibrated and NIST certified mirror (Ocean Optics catalogue #STAN-SSH-NIST).

Fluid Infiltration

Gradual vapor infiltration was done by placing the DBR sample into a closed chamber that presents a quartz window. The chamber was designed to be placed in the optical pathway of the reflectance measurement system described above. Liquid isopropanol is kept in an isolated reservoir and it is introduced in the chamber by a manual valve system that also controls the pressure. As a result of this experimental setup, reflectance spectra can be recorded while the pressure is varied.

Liquid infiltration was made by placing a few drops on top of the surface of the 1DPC and waiting a couple of minutes before measuring. This permits the diffusion through the multilayer structure without the accumulation of liquid on top of the DBR.

Acknowledgements

The research leading to these results has received funding from the European Research Council under the European Union's Seventh Framework Programme (FP7/2007–2013)/ERC grant agreement no. 307081 (POLIGHT), the Spanish Ministry of Economy and Competitiveness under grant MAT2014 54852-R). MA is grateful to "La Caixa" Foundation for its financial support.

Notes and references

1 P. Yeh, Optical Waves in Layered Media, John Wiley & Sons, Hoboken, New Jersey, 2005.
2 G. Kang, J. Yoo, J. Ahn, K. Kim, *Nano Today*, 2015, **10**, 22—47
3 M. Yoshimura, W.L. Suchanek, K. Byrappa, *MRS Bull*. 2000, **25**, 17-25
4 R.M. Almeida, S. Portal, *Curr. Opin. Solid State Mater. Sci.*,2003, **7** , 151–157
5 J. D. Joannopoulos et al. Photonic crystals:molding the flow of light, Princeton University Press, Princeton, 2nd ed., 2008.
6 K. M. Chen, A. W. Sparks, H.C. Luan, D. R. Lim, K. Wada, L. C. Kimerling, *Appl. Phys Lett* 1999, **75**, 3805
7 D.C. Johnson, I. Ballard, K.W.J. Barnham, D.B. Bishnell, J.P. Connolly, M.C. Lynch, T.N.D. Tibbits, N.J. Ekins-Daukes, M. Mazzer, R. Airey, G. Hill, J.S. Roberts, *Sol. Energ. Mat. Sol. C.*, 2005, **87**, 169–179
8 L. Hou, Q. Hou, Y. Mo, J. Peng, Y. Cao, *Applied Phys. Lett.*, 2005, **87**, 243504
9 R. Betancur, P. Romero-Gomez, A. Martinez-Otero, X. Elias, M. Maymó, J. Martorell, *Nat. Photonics*, 2013 , **7**, 995-1000
10 P. Bermel, C. Luo, L. Zeng, L. C. Kimerling, J. D. Joannopoulos, *Opt. Express*, 2007, **15**, 16986-17000.
11 K. Xie, M. Guo, H. Huang, *J. Mater. Chem. C*, 2015, **3**, 10665-10686
12 A. Jiménez-Solano, J.M. Delgado-Sánchez, M.E. Calvo, J.M. Miranda-Muñoz, G. Lozano, D. Sancho, E. Sánchez-Cortezón, H. Míguez, *Prog. Photovolt: Res. Appl.*, 2015, **23**, 1785–1792.
13 H. Shen, Z. Wang, Y. Wu, B. Yang, *RSC Adv*., 2016, **6**, 4505-4520
14 J.J. Steele, A.C. van Popta, M.M. Hawkeye, J.C. Sit, M.J. Brett, *Sens. Actuators B*, 2006, **120**, 213
15 L. Passoni, L. Criante, F. Fumagalli, F. Scotognella, G. Lanzani and F. Di Fonzo, *ACS Nano*, 2014, **8**, 1216
16 M.C. Fuertes, F.J. López-Alcaraz, M.C. Marchi, H.E. Troiani, H. Míguez, G.J.A.A. Soler Illia, *Adv. Funct. Mater*., 2007, **17**, 1247
17 S. Colodrero, M. Ocaña, H. Míguez., *Langmuir,* 2008, **24**, 4430.
18 L. D. Bonifacio, D. P. Puzzo, S. Breslav, B. M. Willey, A. McGeer, G. A. Ozin, *Adv*. *Mater*., 2010, **22**, 1351-1354
19 K. Szendrei, P. Ganter, O. Sánchez-Sobrado, R. Eger, A. Kuhn, B.V. Lotsch, *Adv. Mater.* **2015**, *27*, 6341–634
20 M. Muallem, A. Palatnik, G. D. Nessim, Y. R. Tischler, *ACS Appl. Mater. Interfaces*, 2015, **7**, 474–481
21 M.F. Schubert, J.Q. Xi, J.K. Kim, E.F. Schubert, *Appl. Phys. Lett.*, 2007, **90**, 141115
22 E. J. Anglin, L. Cheng, W. R. Freeman, M.J. Sailor et al., *Adv. Drug. Deliver. Rew*., 2008, **60**,1266
23 M.E. Calvo, S. Colodrero, T.C. Rojas, M. Ocaña, J.A. Anta, H. Míguez*, Adv. Func. Mater.*, 2008, **18**, 2708
24 C. Bronnbauer, J. Hornich, N. Gasparini, F. Guo, B. Hartmeier, N.A. Luechinger, C. Pflaum, C.J. Brabec, K. Forberich, *Adv. Optical Mater.* 2015, **3**, 1424–1430
25 M. E. Calvo, S. Colodrero, N. Hidalgo, G. Lozano, C. Lopez-Lopez, O. Sanchez-Sobrado, H. Miguez, *Energy Environ. Sci.*, 2011, **4**, 4800–481
26 S. Colodrero, A. Mihi, L. Häggman, M. Ocaña, G. Boschloo, A. Hagfeldt, H. Míguez, *Adv. Mater.*, 2009, **21**, 764
27 S. Guldin, M. Kolle, M. Stefik, R. Langford, D. Eder, U. Wiesner, U. Steiner, *Adv. Mater.* 2011, **23**, 3664–3668
28 W. Zhang, M. Anaya, G. Lozano, M. E. Calvo, M. B. Johnston, H. Míguez, H. J. Snaith, *Nano Letters*, 2015, **15**, 1698-1702
29 I. Pavlichenko, E. Broda, Y. Fukuda, K. Szendrei, A. K. Hatz, G. Scarpa, P. Lugli, C. Bräuchle, B. V. Lotsch, *Mater. Horiz.,* 2015, **2**, 299-308
30 L. Frezza*,* M. Patrini*,* M. Liscidini*,* D. Comoretto*, J. Phys. Chem. C,* 2011*,* **115,** 19939
31 F. Scotognella, D.P. Puzzo, A. Monguzzi, D.S. Wiersma, D. Maschke, R. Tubino, G.A. Ozin, *Small*, 2009, **5**, 2048
32 M. Oliva-Ramirez, A. Barranco, M. Löffler, F. Yubero, A. R. González-Elipe, A*CS Nano*, 2016, **10**, 1256
33 (a) M. E. Calvo, N. Hildago, R. Schierholz, A. Kovàcs, A. Fernandez, M. G. Bellino, G. J. A. A. Soler-Illia, H. Miguez, *Nanoscale*, 2015, **7**, 16582-16589 (b) N. Hidalgo, M. E. Calvo, M. G. Bellino, G. J. A. A. Soler-Illia, H. Míguez, *Adv. Func. Mater*., 2011, **21**, 2534-2540

View Article Online
DOI: 10.1039/C6TC00663A

34 W.J. Nimens, L. Whittaker-Brooks, M. H. Bartl, *J. Mater. Chem. C*, 2016, **4**, 668-672
35 B.V. Lotsch, G.A. Ozin, *ACS Nano*, 2008, **2**, 2065
36 B. Brudieu, A. Le Bris, J. Teisseire, f. Guillemont, G. Dantelle, S. Misra, P. Roca i Cabarrocas, F. Sorin, T. Gacoin, *Adv Optical Mater*., 2014, **2**, 1105-1112
37 J.H. Prosser, T. Brugarolas, S. Lee, A. J. Nolte, D. Lee, *Nano Lett.*, 2012, **12**, 5287−5291
38 M. Anaya, M. E. Calvo, J. M. Luque-Raigón, H. Míguez, *J. Am. Chem. Soc.,* 2013, **135**, 7803−7806.
39 Y. Huang, J. T. Park, J. H. Prosser, J. H. Kim, D. Lee, *J. Mater. Chem. C*, 2014, **2**, 3260–3269
40 D. Grosso, C. Boissière, C. Sanchez, *Nat. Mater.* 2007, **6**, 572-575
41 J. Bravo, L. Zhai, Z. Wu, R. E. Cohen,M. F. Rubner, *Langmuir,* 2007, **23**, 7293
42 A. Rehmer, K. Scheurell, E. Kemnitz, *J. Mater. Chem. C*, 2015, **3**, 1716-1723
43 J. Noack, K. Scheurell, E. Kemnitz, P. Garcia-Juan, H. Rau, M. Lacroix, J. Eicher, B. Lintner, T. Sontheimer, T. Hofmann, J. Hegmann, R. Jahn, P. Löbmann, *J. Mater. Chem.* 2012, **22**, 18535
44 P. Kurt, P.; D. Banerjee, R.E. Cohen, M.F. Rubner, *J. Mater.Chem.* 2009, **19**, 8920
45 M. C. Fuertes, M. Marchena, M. C. Marchi, A. Wolosiuk, G. J. A. A. Soler-Illia, *Small* 2009, **5**, 272–280
46 G. Lozano, S. Colodrero, O. Caulier, M.E. Calvo and H. Míguez, *J. Phys. Chem. C.* 2010, **114**, 3681
47 N. Hidalgo, C. López-López, G. Lozano, M. E. Calvo, H. Míguez, *Langmuir*, 2012, **28**, 13777-13782
48 M. E. Calvo and H. Mıguez, in Responsive Photonic Nanostructures:Smart Nanoscale Optical Materials, ed. Y. Yin,The Royal Society of Chemistry, Cambridge, UK, 2013,pp. 1–21.

View Article Online
DOI: 10.1039/C6TC00663A

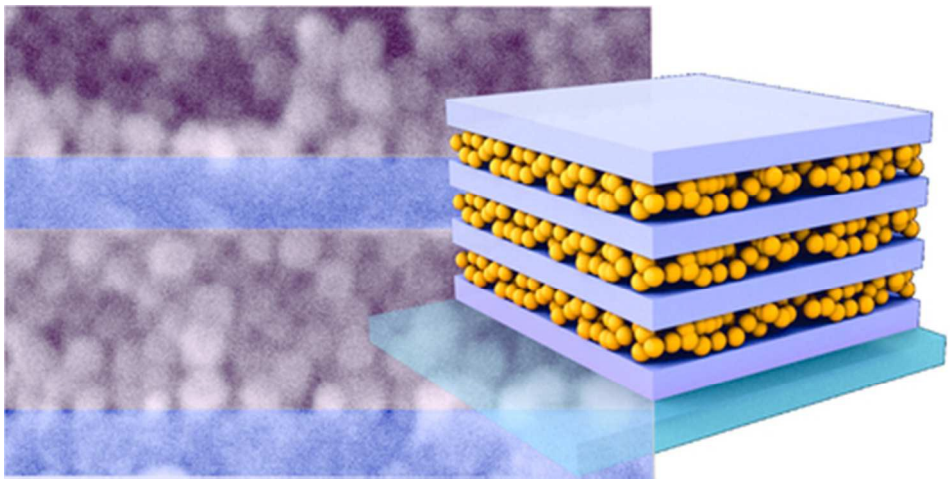

39x19mm (300 x 300 DPI)